Geophysical Research Letters

RESEARCH LETTER
10.1029/2022GL099463

Key Points:

- Global warming reduces ozone in the tropical lower stratosphere, an effect typically attributed to strengthening stratospheric upwelling
- Yet, global warming also deepens the troposphere, which erodes the ozone layer and reduces transport of ozone into the lower stratosphere
- Along with strengthening upwelling, tropospheric expansion contributes at leading order to reductions in tropical lower stratospheric ozone

Supporting Information:

Supporting Information may be found in the online version of this article.

Correspondence to:

A. Match,
aaron.match@nyu.edu

Citation:

Match, A., & Gerber, E. P. (2022). Tropospheric expansion under global warming reduces tropical lower stratospheric ozone. *Geophysical Research Letters*, *49*, e2022GL099463. https://doi.org/10.1029/2022GL099463

Received 5 MAY 2022
Accepted 22 SEP 2022

Author Contributions:

Conceptualization: Aaron Match
Formal analysis: Aaron Match, Edwin P. Gerber
Funding acquisition: Aaron Match
Methodology: Aaron Match, Edwin P. Gerber
Project Administration: Aaron Match
Supervision: Edwin P. Gerber
Visualization: Aaron Match
Writing – original draft: Aaron Match
Writing – review & editing: Aaron Match, Edwin P. Gerber

Tropospheric Expansion Under Global Warming Reduces Tropical Lower Stratospheric Ozone

Aaron Match[1] **and Edwin P. Gerber**[1]

[1]Center for Atmosphere Ocean Science, Courant Institute of Mathematical Sciences, New York University, New York City, NY, USA

Abstract In response to global warming, ozone is predicted to increase aloft due to stratospheric cooling but decrease in the tropical lower stratosphere. The ozone reductions have been primarily attributed to a strengthening Brewer-Dobson circulation, which upwells ozone-poor air. Yet, this paper finds that strengthening upwelling only explains part of the reduction. The reduction is also driven by tropospheric expansion under global warming, which erodes the ozone layer from below, the low ozone anomalies from which are advected upwards. Strengthening upwelling and tropospheric expansion are correlated under global warming, making it challenging to disentangle their relative contributions. Therefore, chemistry-climate model output is used to validate an idealized model of ozone photochemistry and transport with a tropopause lower boundary condition. In our idealized decomposition, strengthening upwelling and tropospheric expansion both contribute at leading order to reducing tropical ozone. Tropospheric expansion drives bottom-heavy reductions in ozone, which decay in magnitude into the mid-stratosphere.

Plain Language Summary The ozone layer absorbs ultraviolet light otherwise harmful to life. Due to compliance with the Montreal Protocol, the ozone layer is generally recovering from depletion. But, at the same time, global warming is predicted to impact ozone, increasing ozone in the upper stratosphere and decreasing ozone in the tropical lower stratosphere. These decreases are typically argued to result from a strengthening of tropical stratospheric upwelling under global warming. Yet, this paper shows that in addition to contributions from strengthening upwelling, much of the ozone loss arises from a deepening of the troposphere under global warming. The deepening of the troposphere erodes the ozone layer from below, with the low ozone anomalies in the eroded region subsequently transported upwards by the background upwelling. Deepening of the troposphere therefore helps to explain the predicted ozone reductions throughout the tropical lower stratosphere.

1. Introduction

Chemistry-climate models robustly predict that, in response to global warming, ozone will increase in the upper stratosphere and decrease in the tropical lower stratosphere (SPARC, 2010). The simulated ozone response to a quadrupling of CO_2 is shown in Figures 1a–1c, using output from chemistry-climate models with interactive ozone chemistry contributed to the Coupled Model Intercomparison Project Phase 6 (CMIP6; Eyring et al., 2016). The robustness of the simulated decrease in tropical lower stratospheric ozone suggests models may capture consistent mechanisms for the change (Chiodo et al., 2018). Global warming might already be reducing ozone in the tropical lower stratosphere, where the recovery since 2000 due to the Montreal Protocol has been notably absent (Petropavlovskikh et al., 2019).

Most mechanistic studies explain the reduction in tropical lower stratospheric ozone as resulting from a strengthening of tropical upwelling associated with the Brewer-Dobson circulation (e.g., Banerjee et al., 2016; Chiodo et al., 2018; Dietmuller et al., 2021; Li et al., 2009; Meul et al., 2014; Oman et al., 2010; Plummer et al., 2010; Shepherd, 2008; SPARC, 2010; Waugh et al., 2009). Strengthened upwelling reduces ozone by transporting ozone-poor air upwards against the climatological gradient. We identify four lines of evidence implicating strengthening upwelling. First, prescribing strengthened upwelling in a chemical transport model (CTM) reduces tropical lower stratospheric ozone (Jiang et al., 2007). Second, the dipole of ozone decreasing in the tropical lower stratosphere while increasing in the extratropical lower stratosphere has been interpreted as a signature of a strengthened Brewer-Dobson circulation (Shepherd, 2008). Third, the sign of ozone changes in the lower stratosphere were found to match the sign of the change in ozone advection (Li et al., 2009). Fourth, across global

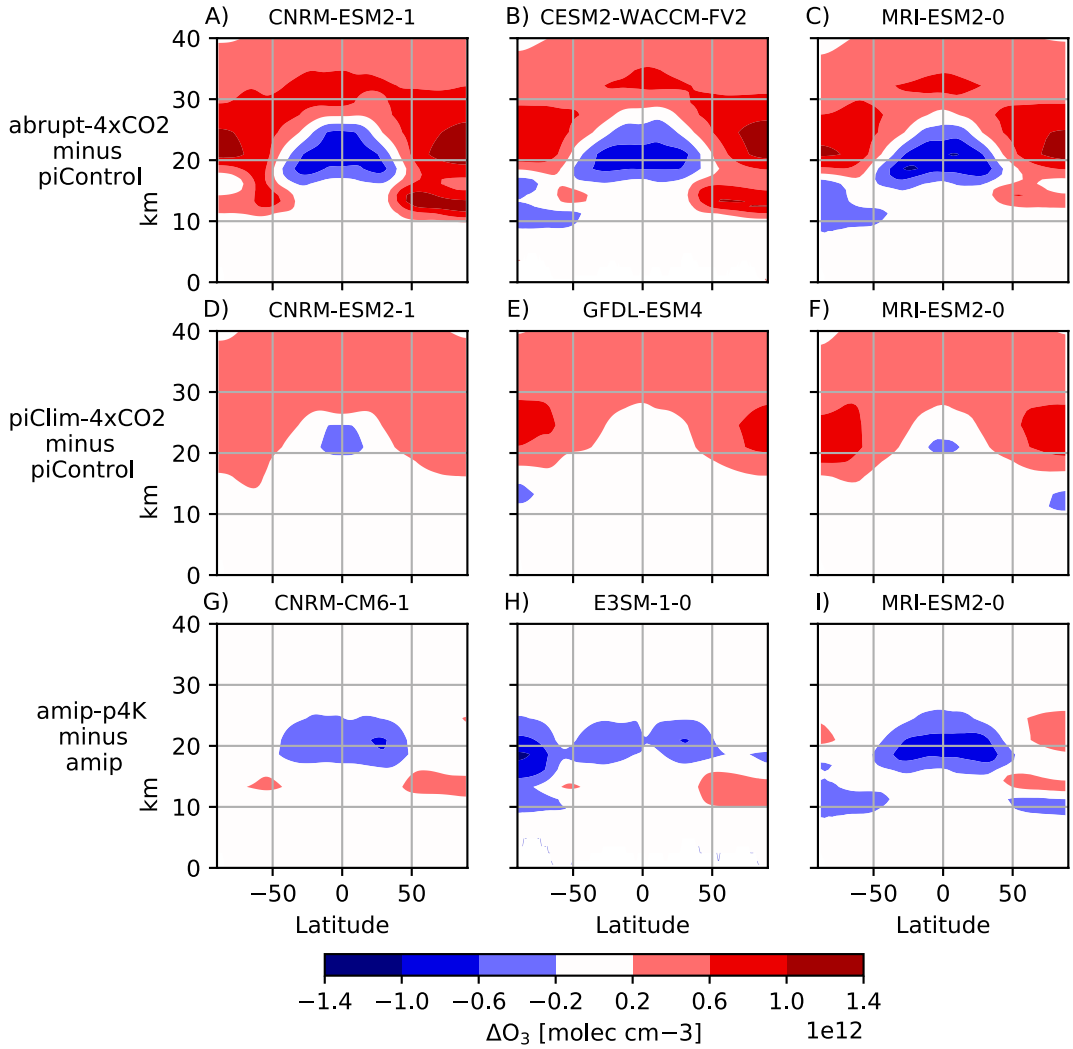

Figure 1. Ozone difference between three pairs of Coupled Model Intercomparison Project Phase 6 experiments. (Top row) Ozone difference between final 100 years of abrupt-4xCO_2 and piControl. (Middle row) Ozone difference between piClim-4xCO_2 and piControl reveals the effect of stratospheric cooling. (Bottom row) Ozone difference between amip-p4K and amip reveals the effect of surface warming. Note that included models vary in each row.

warming simulations, increases in upwelling are correlated with decreases in tropical lower stratospheric ozone (Chiodo et al., 2018; Dietmuller et al., 2021; Oman et al., 2010; SPARC, 2010, Figure 9.6).

Beyond these formidable lines of evidence implicating strengthening upwelling, we propose an additional loss mechanism—expansion of tropospheric ozone destruction. Global warming deepens the troposphere (Match & Fueglistaler, 2021; Singh & O'Gorman, 2012; Vallis et al., 2015), transforming stratospheric air into tropospheric air with a shorter ozone lifetime due to tropospheric chemistry and rapid overturning that facilitates dry deposition at the surface (Wild, 2007). In other words, tropospheric expansion takes a "bite" out of the ozone layer from below. In the tropics, the low-ozone anomalies from the bite are then advected upwards by the background upwelling, smearing the ozone reductions upwards into the tropical lower stratosphere until photochemical equilibrium is reestablished. A related mechanism has been invoked to explain the ozone annual cycle in the tropical tropopause layer (Folkins et al., 2006), but this mechanism has not been invoked to explain the response to global warming.

The goal of this study is to evaluate whether tropospheric expansion contributes at leading order to ozone reductions in the tropical lower stratosphere under global warming. Comprehensive model experiments will be used to examine the ozone response to a quadrupling of CO_2, and that response will be decomposed into ozone responses

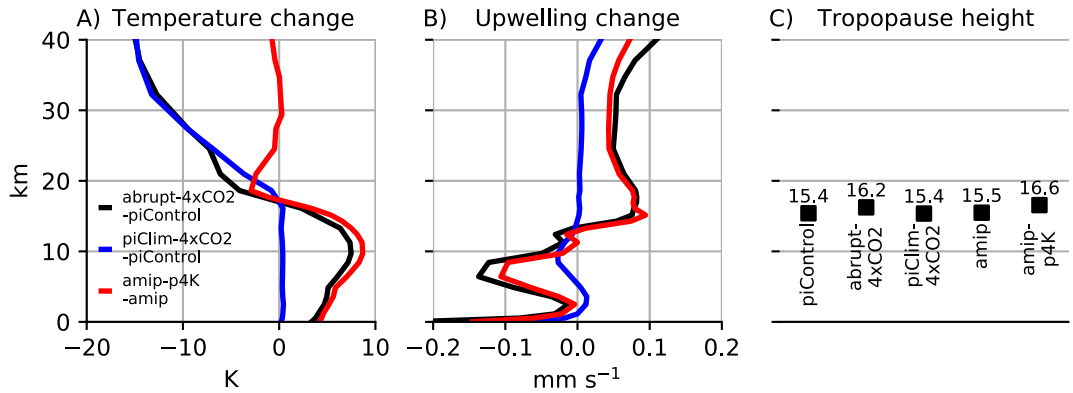

Figure 2. Dynamical changes relevant to ozone response in MRI-ESM2-0. (a) Temperature difference between pairs of experiments. (b) Residual upwelling difference between pairs of experiments. (c) Tropopause height (WMO definition of thermal tropopause) in each experiment, with exact values noted. Quantities are averaged over the tropics from 30°S to 30°N.

to stratospheric cooling and surface warming. When further insights from CMIP6 are stymied by correlations between upwelling and tropopause height, we will analyze an idealized model of ozone photochemistry and transport to further decompose the relative roles of strengthening upwelling and tropospheric expansion.

2. Chemistry-Climate Model Results

The ozone response to global warming is proposed to involve three mechanisms: (a) stratospheric cooling, (b) strengthening upwelling, and (c) tropospheric expansion (scrutinized herein). We analyze these mechanisms in comprehensive chemistry-climate models contributed to CMIP6 (Eyring et al., 2016). Features that are robust across models are treated as predictions worth understanding, as in previous studies (e.g., Chiodo et al., 2018), even though models could have limitations stemming from limited resolution or sub-grid parameterizations. Figures 1a–1c compare ozone under abrupt quadrupling of CO_2 (abrupt-4xCO_2) with the pre-industrial control (piControl), showing well-reported increases throughout the upper stratosphere but decreases in the tropical lower stratosphere (e.g., Chiodo et al., 2018).

All three mechanisms are expected to be simulated self-consistently in response to global warming, so additional information is needed to decompose the mechanisms of the ozone response. We gather such information from mechanism denial experiments, in which the ozone response to greenhouse gas forcing is decomposed into (a) the response to quadrupling of CO_2 at fixed surface temperature, and (b) the response to surface warming at prescribed CO_2 concentrations. A similar decomposition was performed by Fomichev et al. (2007). Our results provide the first intermodel comparison of such mechanism denial experiments.

2.1. Ozone Response at Fixed Surface Temperature

The ozone response at fixed surface temperature is diagnosed by comparing an experiment with quadrupled CO_2 but prescribed pre-industrial sea surface temperature (piClim-4xCO_2) to the pre-industrial control experiment (piControl). The piClim-4xCO_2 experiments were conducted as part of the Radiative Forcing Model Intercomparison Project (RFMIP; Pincus et al., 2016), and we analyze CNRM-ESM2-1, GFDL-ESM4, and MRI-ESM2-0. Figures 1d–1f show the ozone responses. Even at fixed surface temperature, the stratosphere cools directly from the greenhouse gas forcing (Manabe et al., 1967). Stratospheric cooling increases ozone aloft by slowing ozone chemical loss reactions (e.g., Jacob, 1999).

These experiments exhibit minor reductions in ozone in the tropical lower stratosphere, our region of interest. These reductions are typically understood to arise from "reverse self-healing," whereby the anomalously increased ozone aloft absorbs ultraviolet photons that would have otherwise formed ozone in the lower stratosphere (Groves et al., 1978; Haigh & Pyle, 1982; Jonsson et al., 2004). Figure 2 compares the dynamical and thermodynamical environments in these suites of experiments, highlighting which variables are likely to drive the ozone response. Figure 2a confirms that, at fixed surface temperature, the stratosphere cools substantially in

response to quadrupling of CO_2, with minimal changes in upwelling (Figure 2b) or tropopause height (Figure 2c). Ozone reductions in the tropical lower stratosphere remain small without strengthened upwelling or tropospheric expansion.

2.2. Ozone Response to Prescribed Surface Warming

The ozone response to surface warming is diagnosed by comparing historical simulations with prescribed sea surface temperatures subject to a warming of 4 K (amip-p4K) versus historical simulations with no additional warming (amip). The amip-p4K experiments were conducted as part of the Cloud Feedback Model Intercomparison Project (Webb et al., 2017), and we analyze CNRM-CM6-1, E3SM-1-0, and MRI-ESM2-0. Figures 1g–1i show this ozone response to prescribed surface warming. Surface warming reduces ozone in the tropical lower stratosphere while barely perturbing ozone aloft.

Figure 2a shows that there is minimal stratospheric temperature change in response to prescribed surface warming (red), so there is little ozone change from temperature-dependent chemistry. The prevailing explanation for how surface warming reduces tropical lower stratospheric ozone is that it strengthens the upwelling of ozone-poor air from below. Indeed, prescribing surface warming reproduces the full strengthening of the Brewer-Dobson circulation from the quadrupled CO_2 case (Figure 2b, black and red curves). Yet, at the same time, the troposphere deepens in response to surface warming (from 15.5 km in the amip experiment to 16.6 km in the amip-p4K for MRI-ESM2-0), comparable to the 1 km by which the tropopause deepens upon a quadrupling of CO_2 (from 15.4 km in piControl to 16.2 km in abrupt-4xCO_2 for MRI-ESM2-0).

Because surface warming simultaneously strengthens upwelling and deepens the troposphere, these experiments cannot facilitate a decomposition of the relative roles of strengthening upwelling and tropospheric expansion. We therefore formulate a model in which tropopause height can be held fixed while increasing upwelling, and vice versa.

3. The Idealized Model: Formulation

Our idealized model couples together a tropical and extratropical column, each undergoing Chapman photochemistry, transport via a leaky tropical pipe, and tropopause lower boundary conditions. The model predicts the annual, spatial mean ozone concentration in the tropics $[O_3]_T$ and the extratropics $[O_3]_E$. The prognostic equations for ozone number density [units: molec cm^{-3}] are as follows:

$$\frac{\partial [O_3]_i}{\partial t} = \frac{\partial [O_3]_i}{\partial t}\Big|_{\text{photochemistry}} + \frac{\partial [O_3]_i}{\partial t}\Big|_{\text{transport}} \quad (1)$$

where subscript i corresponds to tropics (T) or extratropics (E):

3.1. Photochemistry

Ozone photochemistry is represented by the paradigmatic Chapman cycle (Chapman, 1930), following the treatment of Jacob (1999). Chapman photochemistry considers the evolution of three oxygen species (O, O_2, and O_3):

$$O_2 + h\nu \rightarrow O + O \qquad (\lambda < 240\text{nm}) \qquad \text{(R1)}$$

$$O + O_2 + M \rightarrow O_3 + M \qquad \text{(R2)}$$

$$O_3 + h\nu \rightarrow O_2 + O \qquad (\lambda < 320\text{nm}) \qquad \text{(R3)}$$

$$O_3 + O \rightarrow 2O_2 \qquad \text{(R4)}$$

where M represents third bodies with the number density of air molecules. Following textbook treatments, reactions 2 and 3 proceed quickly, so ozone evolves slowly as follows:

$$\frac{\partial [O_3]}{\partial t}\Big|_{\text{photochemistry}} = 2k_1 C_{O_2} n_a - \frac{2k_3 k_4}{k_2 C_{O_2} n_a^2}[O_3]^2 \quad (2)$$

where C_{O_2} is the molar fraction of O_2 in air (today, 0.21), and $n_a(z)$ is the number density of air [molec cm^{-3}] decaying exponentially over $H = 7$ km.

The photolysis rate constants k_1 and k_3 depend on radiation interacting with O_2 and O_3. The photolysis rates are calculated by integrating the spectrally resolved photolysis rate:

$$k = \int_{\lambda} q(\lambda)\sigma(\lambda)I_{\lambda}d\lambda \tag{3}$$

with wavelength λ [nm], quantum yield q (molecules produced per photon absorbed), absorption coefficient σ (cm^2 molec^{-1}), and actinic flux density with respect to wavelength I_λ (photons cm^{-2} s^{-1} nm^{-1}). The actinic flux is a radiative quantity dependent on absorption above:

$$I_{\lambda}(z) = I_{\lambda,\infty}\exp\left(-\frac{\tau_{\lambda}(z)}{\cos\,\theta}\right) \tag{4}$$

where τ_λ is the wavelength-dependent optical depth resulting from absorption by chemical species aloft and θ is the solar zenith angle. We consider overhead sun in the tropics ($\theta = 0°$) and low sun in the extratropics ($\theta = 60°$). Only absorption by O_2 and O_3 is considered:

$$\tau_{\lambda}(z) = \int_{z}^{\infty}\left(\sigma_{O_2}(\lambda)\,[O_2] + \sigma_{O_3}(\lambda)\,[O_3]\right)dz' \tag{5}$$

Temperature-dependent rate constants k_2 and k_4 are calculated as in Brasseur and Solomon (2005). Analytical solutions of the equilibrium ozone profile do not exist for Chapman photochemistry because the radiation that forms ozone is a function of the ozone profile itself. The ozone equilibrium is found numerically, also accounting for transport.

3.2. Transport

Ozone is transported between the tropics and extratropics by advection and mixing, a leaky tropical pipe (Neu & Plumb, 1999; Plumb, 1996) following the treatment of Stolarski et al. (2014).

$$\frac{\partial\,[O_3]_T}{\partial t}\Big|_{\text{transport}} = -wn_a\frac{\partial}{\partial z}\left(\frac{[O_3]_T}{n_a}\right) - \mu\,([O_3]_T - [O_3]_E) \tag{6}$$

$$\frac{\partial\,[O_3]_E}{\partial t}\Big|_{\text{transport}} = wn_a\frac{\partial}{\partial z}\left(\frac{[O_3]_E}{n_a}\right) + (D+\mu)\,([O_3]_T - [O_3]_E) \tag{7}$$

where w is the rate of upwelling/downwelling (default: 0.3 mm s^{-1}), μ is the lateral mixing rate between the tropics and extratropics (1 year^{-1}), and D (units: s^{-1}) is the mass flux divergence of the tropical upwelling.

$$D = -e^{z/H}\frac{\partial}{\partial z}\left(we^{-z/H}\right) \tag{8}$$

The mass flux divergence of the upwelling in the tropics transports ozone to the extratropics.

3.3. Tropopause Boundary Conditions

The tropopause is approximated as a zero-ozone lower boundary for the stratosphere in each column, reflecting the fast tropospheric destruction of ozone through chemical sinks and dry deposition facilitated by the rapid overturning of the troposphere (e.g., Wild, 2007). Increases in tropopause height destroy stratospheric ozone by converting stratospheric air into zero-ozone tropospheric air. Increases in tropopause height also lift the zero-ozone boundary condition for ozone transport, reducing ozone in the interior of the domain. By default, the tropical tropopause is at 17 km and the extratropical tropopause is at 10 km.

3.4. Model Set-Up and Parameters

The idealized shortwave radiative transfer and photolysis rates are solved on a wavelength grid with 141 discretized wavelengths ranging from 180 to 320 nm. The default temperature is uniformly 240 K. O_2 absorption coefficients $\left(\sigma_{O_2}\right)$ are taken from Ackerman (1971) and O_3 absorption coefficients $\left(\sigma_{O_3}\right)$ from Demore et al. (1997). Solar actinic flux is calculated from the Solar Spectral Irradiance Climate Data Record (Coddington et al., 2015), averaged from 01 January 2020 to 02 April 2021. Spectrally resolved parameters are linearly interpolated to the wavelength grid.

The vertical dimension is discretized into vertical levels ($\Delta z = 500$ m) ranging from the tropopause to 40 km. The timestep is 10,000 s, and the model is run to approximate equilibrium for 50,000 time steps (roughly 15 years).

Chapman photochemistry is known to simulate roughly double the observed ozone concentration, due to neglected catalytic destruction from NO_x and HO_x (e.g., Jacob, 1999, as observed in our model in Figure S1 in Supporting Information S1). Incorporating catalytic chemistry can increase the number of chemical reactions by an order of magnitude (Crutzen, 1971), yet our results suggest these reactions are not necessary to explain leading-order aspects of the ozone response to global warming. By neglecting catalytic chemistry, our idealized model trades off the quantitative accuracy of more complex models while distilling the essential mechanisms of the ozone response to global warming.

4. The Idealized Model: Validation and Results

Because idealized Chapman photochemistry overestimates basic state ozone, we need to determine whether our idealized model nonetheless possesses realistic sensitivity to quadrupling CO_2. We impose a CO_2 quadrupling through three idealized perturbations resembling the responses in MRI-ESM2-0 (Figure 2): stratospheric cooling of 10 K, strengthened upwelling of 0.05 mm s^{-1}, and tropospheric expansion of 1 km. We focus on whether tropospheric expansion contributes at leading order to tropical lower stratospheric ozone reductions.

The idealized model response to these perturbations is shown in Figure 3b (black curve), as compared to the comprehensive CMIP6 results in Figure 3a. The idealized model reproduces the order of magnitude of the ozone changes as well as the vertical structure, with increases aloft and decreases below (compare the black curve in Figure 3b to each curve in Figure 3a). This agreement builds confidence that the idealized model is producing a reasonable representation of the emergent ozone dynamics. We further validate the idealized model by reproducing the response to stratospheric cooling in Figure 3d. The idealized response to stratospheric cooling reproduces the modest ozone reductions from reverse self-healing, although it overestimates the ozone increase aloft by roughly a factor of two. In addition, we use the idealized model to reproduce the response to surface warming (Figure 3f vs. Figure 3e). In both the chemistry-climate models and our idealized model, reductions in tropical lower stratospheric ozone are primarily driven by surface warming. The idealized model results do not change much when realistic temperature and upwelling are used in the basic state and for the global warming perturbations, as shown in Figure S2 in Supporting Information S1. Although the idealized model appears fit for our analysis, its details are likely sensitive to the overestimated ozone in its basic state (Figure S1 in Supporting Information S1), which could inflate its sensitivity to both strengthening upwelling and tropospheric expansion.

Having built confidence in the idealized model, we turn to its key purpose: decomposing the relative contributions of strengthening upwelling and tropospheric expansion. This decomposition can be seen in Figures 3b and 3f. Strengthening upwelling (magenta) leads to ozone decreases throughout the tropical lower stratosphere, as expected from its advection against the climatological gradient of increasing ozone in this region. Strengthening upwelling induces large ozone anomalies in the lower stratosphere, where transport is fast compared to photochemical recovery timescales (years around 23 km and months around 28 km; Dutsch, 1968; Jacob, 1999). Strengthening upwelling barely perturbs ozone in the upper stratosphere, where transport is slow compared to photochemical recovery timescales (weeks around 33 km and days around 38 km).

Although absent from previous explanations, tropospheric expansion plays a leading order role, too (Figure 3f, red). This is our main result. Mechanistically, tropospheric expansion destroys ozone by transforming stratospheric air into tropospheric air with a shorter ozone lifetime, that is, "taking a bite" out of the stratosphere. The anomalies from the bite are then advected upwards by the background upwelling into regions where photochemical

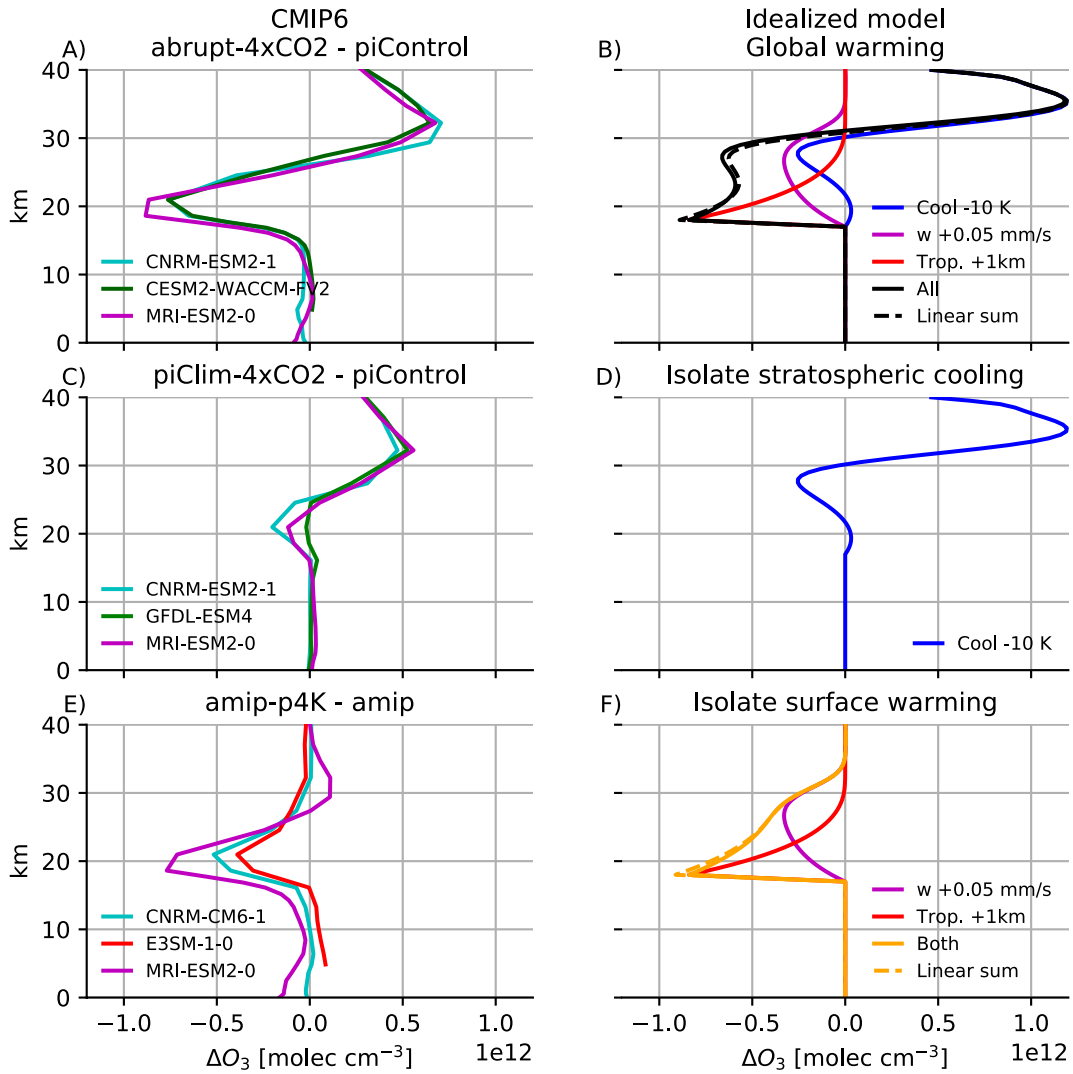

Figure 3. (Left column) Tropically averaged ozone change in Coupled Model Intercomparison Project Phase 6 (CMIP6) experiments and (right column) idealized model response decomposed into relevant mechanisms. (a) Ozone responses to quadrupled CO_2 in CMIP6. (b) Idealized model response to perturbations analogous to quadrupled CO_2, that is, stratospheric cooling of 10 K (blue), strengthened upwelling of 0.05 mm s^{-1} (magenta), and tropospheric expansion of 1 km (red), all perturbations together (black), and their linear sum (dashed black). (c) Ozone responses to quadrupled CO_2 at fixed surface temperature. (d) Idealized model response to stratospheric cooling. (e) Ozone responses to increased surface temperature by 4 K. (f) Idealized model response to strengthening upwelling (magenta), tropospheric expansion (red), both (orange), and their linear sum (dashed orange). Ozone reductions are driven at leading order by strengthening upwelling (magenta) and tropospheric expansion, which leads to bottom-heavy reductions (red) (panels b and f).

equilibrium is eventually re-established. These advected anomalies that are smeared out through the lower stratosphere add up to a much larger column ozone anomaly than what was formed by the bite itself. In other words, the integral of the red curve in Figure 3b is dominated by the region above 18 km (the advected anomalies) compared to the region from 17 to 18 km (the bite). Figure 4 illustrates this two-step (bite then advect) mechanism. The change in column ozone is the same in response to the perturbations to upwelling versus tropopause height used in our idealized experiments, but the main result is that these processes both contribute at leading order.

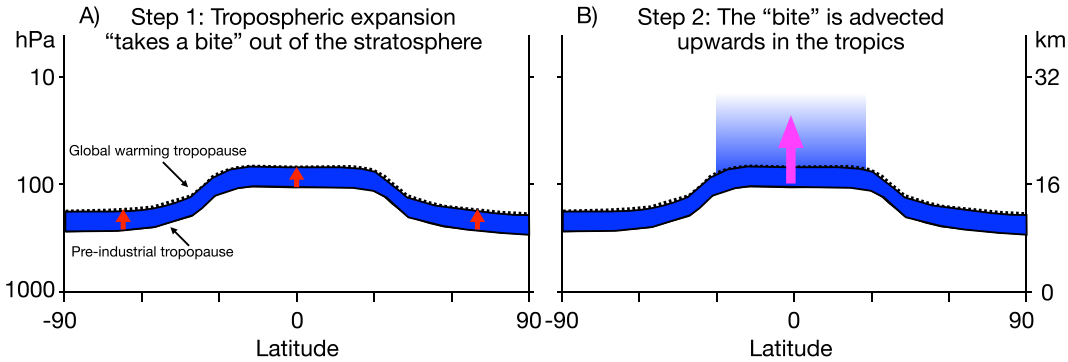

Figure 4. Cartoon illustrating the impact of expansion of tropospheric destruction of ozone. (a) Tropospheric expansion "takes a bite" out of the stratosphere by converting stratospheric air to tropospheric air. (b) The "bite" is advected upwards in the tropics by the background Brewer-Dobson circulation until photochemical equilibrium is gradually re-established.

5. Discussion

5.1. Does Ozone Shift Upwards?

Tropopause height has long been known to influence ozone. At synoptic scales, mid-latitude storms redistribute ozone laterally and vertically, leading to correlations between column ozone and tropopause height (Appenzeller et al., 2000; Meetham & Dobson, 1937; Reed, 1950; Schubert & Munteanu, 1988). Steinbrecht et al. (1998) speculated that these synoptic correlations might extend to decadal scales. At these longer timescales, Forster and Tourpali (2001) attempted to remove the dynamical component of tropopause height variations by analyzing ozone trends in tropopause-following coordinates. Thompson et al. (2021) and Bognar et al. (2022) used a similar approach in the tropical lower stratosphere. This method is based on the idea that tropospheric expansion leads to an upward shift of stratospheric ozone. Yet, physically, tropospheric expansion leads to an upward shift in the tropospheric destruction of ozone, not to an upward shift in ozone itself. The ozone response will only resemble a vertical shift where ozone is controlled by upwelling, which excludes the extratropics, which are downwelling, and the upper stratosphere, which is in photochemical equilibrium (Figures S3e and S3f in Supporting Information S1). Because ozone does not shift uniformly upwards with the tropopause, tropopause-following coordinates do not generally remove the effects of tropospheric expansion. Although a uniform shift is not expected from tropospheric expansion, the tropical ozone response to quadrupling of CO_2 strongly resembles a vertical shift predicted from tropospheric expansion, with decreased ozone below and increased ozone aloft (Figures S3a and S3b in Supporting Information S1). But, this increased ozone aloft results from stratospheric cooling, so the resemblance to a vertical shift driven by tropospheric expansion is coincidental.

5.2. Revisiting the Case for Strengthening Upwelling

We now revisit the four lines of evidence implicating strengthening upwelling. Many correctly noted that strengthening upwelling plays a role in reducing ozone, but (sometimes knowingly) did not preclude a role for other mechanisms. First, in the cogent study of Jiang et al. (2007), it was shown that enhancing the Brewer-Dobson circulation in a chemical transport model (CTM) reduced tropical lower stratospheric ozone. Jiang et al. (2007) did not claim that their results precluded other mechanisms.

Second, the ozone reductions in the tropical lower stratosphere and increases in the extratropical lower stratosphere have been implicated as a fingerprint of a strengthened Brewer-Dobson circulation (Shepherd, 2008). Yet, Figure 1 shows that the ozone reductions in the tropics result from surface warming (bottom row), whereas the ozone increases in the extratropics result from stratospheric cooling (middle row). Ozone increases in the extratropical lower stratosphere likely arise from background downwelling of the increased ozone from stratospheric cooling.

Third, Li et al. (2009) reported that the sign of ozone changes in the lower stratosphere matched the change in the ozone tendencies due to advection, suggesting that ozone reductions resulted from strengthening upwelling. However, tropospheric expansion also reduces ozone advection by modifying the boundary conditions on ozone

transport, potentially altering the ozone gradients. Local budgets cannot disentangle the effects of strengthening upwelling from tropospheric expansion.

Fourth, across models, greater strengthening of upwelling correlates with greater reductions in tropical lower stratospheric ozone (Chiodo et al., 2018; Dietmuller et al., 2021; Oman et al., 2010; SPARC, 2010, Figure 9.6). This correlation was claimed to implicate strengthening upwelling. However, this correlation does not reveal causation because strengthening upwelling and tropospheric expansion are both mediated by surface warming (Abalos et al., 2021; Butchart, 2014; Oberländer-Hayn et al., 2016). Indeed, Chiodo et al. (2018) noted that models with the largest upwelling response also had the largest tropospheric warming.

5.3. Relevance to Recent Trends

The contribution of tropospheric expansion to reductions in tropical lower stratospheric ozone appears to be approximately linear with respect to surface warming. In MRI-ESM2-0, the time-dependent ozone response in a 1pctCO_2 experiment grows with global average surface temperature anomaly exactly as predicted by linearly interpolating the response under abrupt-4xCO_2 (Figure S4 in Supporting Information S1). Furthermore, tropospheric expansion is linear with respect to surface warming (as shown in GCMs by Match & Fueglistaler, 2021, their Figure 1), and the column ozone response is linear with respect to tropospheric expansion in the idealized model (Figure S5 in Supporting Information S1). Radiosonde data and reanalyses indicate that the troposphere is expanding at a rate roughly consistent with expectations from global warming, although with spatial heterogeneity and contributions from other factors such as ozone depletion (Meng et al., 2021; Santer et al., 2003; Seidel & Randel, 2006; Xian & Homeyer, 2019). The linearity of the response suggests that roughly a quarter of the 4xCO_2 and amip-p4K scenarios could be relevant to present with a warming of 1 K. A definitive attribution statement is beyond the scope of this work and would need to disentangle additional contributions from internal variability and ozone-depleting substances (Abalos et al., 2019; Dietmuller et al., 2021; Petropavlovskikh et al., 2019; Polvani et al., 2018). In particular, halogen-induced ozone depletion can increase tropical upwelling without causing a surface-mediated change in tropopause height, increasing the relevance of upwelling to date.

6. Conclusions

Chemistry-climate models predict that, in response to increased CO_2, ozone increases in the upper stratosphere due to stratospheric cooling but decreases in the tropical lower stratosphere (Chiodo et al., 2018; Groves et al., 1978; Haigh & Pyle, 1982). The ozone reductions have previously been attributed to strengthening upwelling, which advects ozone-poor air from below (e.g., Banerjee et al., 2016; Chiodo et al., 2018; Dietmuller et al., 2021; Li et al., 2009; Meul et al., 2014; Oman et al., 2010; Plummer et al., 2010; Shepherd, 2008; SPARC, 2010; Waugh et al., 2009). This study also implicates tropospheric expansion, which erodes the ozone layer from below, the low ozone anomalies from which are advected upwards by the background upwelling. Changes in tropopause height and upwelling are correlated in chemistry-climate models under global warming. We constructed an idealized model to separate them, showing that both contribute at leading order to ozone reductions in the tropical lower stratosphere.

These results facilitate new understanding of the ozone response to global warming, highlighting potentially under-emphasized sources of uncertainty when predicting ozone and interpreting ozone trends. Whereas the previous global warming mechanism singularly emphasized the Brewer-Dobson circulation, biases in which could arise from wave dissipation and numerical diffusion in the stratosphere, our results highlight the additional role of tropospheric processes. Convective parameterizations, in particular, could lead to bias both through their impact on transport (vertical advection, mixing) and through differences in the tropopause height perturbation for a given surface warming.

Data Availability Statement

O2 absorption coefficients from Ackerman (1971) accessed from https://uv-vis-spectral-atlas-mainz.org/uvvis/cross_sections/Oxygen/O2.spc Ackerman (1971) 298K_116.3–243.9 nm (int-c).txt. O3 absorption coefficients from Demore et al. (1997), accessed from http://satellite.mpic.de/spectral_atlas/cross_sections/Ozone/O3_JPL-2002(2002)_273K_175-363nm(rec).txt. Solar actinic flux from Coddington et al. (2015) accessed from

https://www.ncei.noaa.gov/products/climate-data-records/solar-spectral-irradiance. CMIP6 data is accessible from https://esgf-node.llnl.gov/search/cmip6/, from which we analyzed Seferian (2018a), Seferian (2018b, 2019); Danabasoglu (2019, 2020), Yukimoto et al. (2019a, 2019b, 2019c, 2019d, 2019e), Krasting et al. (2018), Paynter et al. (2018), Voldoire (2019b, 2019a), Bader et al. (2019), Qin et al. (2021).

Acknowledgments
A.M. acknowledges productive discussions with Stephan Fueglistaler and Nadir Jeevanjee. The authors acknowledge constructive reviews from Susan Solomon, Stephen Bourguet, and an anonymous reviewer. This material is based upon work supported by the National Science Foundation under Award No. 2120717 and OAC-2004572. For the CMIP6 model output, we acknowledge the World Climate Research Programme, the climate modeling groups, and the Earth System Grid Federation (ESGF), as supported by multiple funding agencies.

References

Abalos, M., Calvo, N., Benito-Barca, S., Garny, H., Hardiman, S. C., Lin, P., et al. (2021). The Brewer-Dobson circulation in CMIP6. *Atmospheric Chemistry and Physics*, *21*(17), 13571–13591. https://doi.org/10.5194/ACP-21-13571-2021

Abalos, M., Polvani, L., Calvo, N., Kinnison, D., Ploeger, F., Randel, W., & Solomon, S. (2019). New insights on the impact of ozone-depleting substances on the Brewer-Dobson circulation. *Journal of Geophysical Research: Atmospheres*, *124*(5), 2435–2451. https://doi.org/10.1029/2018jd029301

Ackerman, M. (1971). Ultraviolet solar radiation related to mesospheric processes (Vol. *149*). https://doi.org/10.1007/978-94-010-3114-1_11

Appenzeller, C., Weiss, A. K., & Staehelin, J. (2000). North Atlantic Oscillation modulates total ozone winter trends. *Geophysical Research Letters*, *27*(8), 1131–1134. https://doi.org/10.1029/1999gl010854

Bader, D. C., Leung, R., Taylor, M., & McCoy, R. B. (2019). E3SM-project E3SM1.0 model output prepared for CMIP6 CMIP AMIP. *Earth System Grid Federation*. https://doi.org/10.22033/ESGF/CMIP6.4492

Banerjee, A., Maycock, C., Archibald, A. T., Luke Abraham, N., Telford, P., et al. (2016). Drivers of changes in stratospheric and tropospheric ozone between year 2000 and 2100. *Atmospheric Chemistry and Physics*, *16*(5), 2727–2746. https://doi.org/10.5194/ACP-16-2727-2016

Bognar, K., Tegtmeier, S., Bourassa, A., Roth, C., Warnock, T., Zawada, D., & Degenstein, D. (2022). Stratospheric ozone trends for 1984–2021 in the SAGE II-OSIRIS-SAGE III/ISS composite dataset. *Atmospheric Chemistry and Physics*, *22*(14), 9553–9569. https://doi.org/10.5194/ACP-22-9553-2022

Brasseur, G. P., & Solomon, S. (2005). *Aeronomy of the middle atmosphere: Chemistry and physics of the stratosphere and mesosphere* (3rd edn). Springer.

Butchart, N. (2014). The Brewer-Dobson circulation. *Reviews of Geophysics*, *52*(2), 157–184. https://doi.org/10.1002/2013rg000448

Chapman, S. (1930). A theory of upper atmospheric ozone. *Royal Meteorological Society*, *III*(26), 103–125. Retrieved from https://www.rmets.org/sites/default/files/chapman-memoirs.pdf

Chiodo, G., Polvani, L. M., Marsh, D. R., Stenke, A., Ball, W., Rozanov, E., et al. (2018). The response of the ozone layer to quadrupled CO_2 concentrations. *Journal of Climate*, *31*(10), 3893–3907. https://doi.org/10.1175/jcli-d-17-0492.1

Coddington, O., Lean, J., Lindholm, D., Pilewskie, P., & Snow, M. (2015). *NOAA climate data Record (CDR) of solar spectral irradiance (SSI), version 2.1*. NOAA CDR Program. https://doi.org/10.7289/V53776SW

Crutzen, P. J. (1971). Ozone production rates in an oxygen-hydrogen-nitrogen oxide atmosphere. *Journal of Geophysical Research*, *76*(30), 7311–7327. https://doi.org/10.1029/jc076i030p07311

Danabasoglu, G. (2019). Ncar cesm2-waccm-fv2 model output prepared for CMIP6 CMIP picontrol. *Earth System Grid Federation*. https://doi.org/10.22033/ESGF/CMIP6.11302

Danabasoglu, G. (2020). NCAR CESM2-WACCM-FV2 model output prepared for CMIP6 CMIP abrupt-4xCO_2. *Earth System Grid Federation*. https://doi.org/10.22033/ESGF/CMIP6.11286

Demore, W. B., Howard, C. J., Sander, S. P., Ravishankara, A. R., Golden, D. M., Kolb, C. E., et al. (1997). *Chemical kinetics and photochemical data for use in stratospheric modeling evaluation number 12 NASA panel for data evaluation* (Tech. Rep.). Jet Propulsion Laboratory. Retrieved from https://jpldataeval.jpl.nasa.gov/pdf/Atmos97{_}Anotated.pdf

Dietmuller, S., Garny, H., Eichinger, R., & Ball, W. (2021). Analysis of recent lower-stratospheric ozone trends in chemistry climate models. *Atmospheric Chemistry and Physics*, *21*(9), 6811–6837. https://doi.org/10.5194/ACP-21-6811-2021

Dutsch, H. U. (1968). The photochemistry of stratospheric ozone. *Royal Meteorological Society*, *94*(402), 483–497. https://doi.org/10.1002/qj.49709440205

Eyring, V., Bony, S., Meehl, G. A., Senior, C. A., Stevens, B., Stouffer, R. J., & Taylor, K. E. (2016). Overview of the Coupled Model Intercomparison Project Phase 6 (CMIP6) experimental design and organization. *Geoscientific Model Development*, *9*(5), 1937–1958. https://doi.org/10.5194/GMD-9-1937-2016

Folkins, I., Bernath, P., Boone, C., Lesins, G., Livesey, N., Thompson, A. M., et al. (2006). Seasonal cycles of O_3, CO, and convective outflow at the tropical tropopause. *Geophysical Research Letters*, *33*(16), L16802. https://doi.org/10.1029/2006gl026602

Fomichev, V. I., Jonsson, A. I., de Grandpré, J., Beagley, S. R., McLandress, C., Semeniuk, K., & Shepherd, T. G. (2007). Response of the middle atmosphere to CO_2 doubling: Results from the Canadian middle atmosphere model. *Journal of Climate*, *20*(7), 1121–1144. https://doi.org/10.1175/jcli4030.1

Forster, P. M. F., & Tourpali, K. (2001). Effect of tropopause height changes on the calculation of ozone trends and their radiative forcing. *Journal of Geophysical Research*, *106*(D11), 12241–12251. https://doi.org/10.1029/2000JD900813

Groves, K. S., Mattingly, S. R., & Tuck, A. F. (1978). Increased atmospheric carbon dioxide and stratospheric ozone. *Nature*, *273*(5665), 711–715. https://doi.org/10.1038/273711a0

Haigh, J. D., & Pyle, J. A. (1982). Ozone perturbation experiments in a two-dimensional circulation model. *Quarterly Journal of the Royal Meteorological Society*, *108*(457), 551–574. https://doi.org/10.1002/qj.49710845705

Jacob, D. (1999). *Introduction to atmospheric chemistry*. Princeton University Press. Retrieved from http://acmg.seas.harvard.edu/people/faculty/djj/book/

Jiang, X., Eichelberger, S. J., Hartmann, D. L., Shia, R., & Yung, Y. L. (2007). Influence of doubled CO_2 on ozone via changes in the Brewer–Dobson circulation. *Journal of the Atmospheric Sciences*, *64*(7), 2751–2755. https://doi.org/10.1175/jas3969.1

Jonsson, A. I., de Grandpré, J., Fomichev, V. I., McConnell, J. C., & Beagley, S. R. (2004). Doubled CO_2 -induced cooling in the middle atmosphere: Photochemical analysis of the ozone radiative feedback. *Journal of Geophysical Research*, *109*(D24), D24103. https://doi.org/10.1029/2004jd005093

Krasting, J. P., John, J. G., Blanton, C., McHugh, C., Nikonov, S., Radhakrishnan, A., et al. (2018). NOAA-GFDL GFDL-ESM4 model output prepared for CMIP6 CMIP picontrol. *Earth System Grid Federation*. https://doi.org/10.22033/ESGF/CMIP6.8669

Li, F., Stolarski, R. S., & Newman, P. A. (2009). Stratospheric ozone in the post-CFC era. *Atmospheric Chemistry and Physics*, *9*(6), 2207–2213. https://doi.org/10.5194/ACP-9-2207-2009

Manabe, S., Wetherald, R. T., Manabe, S., & Wetherald, R. T. (1967). Thermal equilibrium of the atmosphere with a given Distribution of relative humidity. *Journal of the Atmospheric Sciences*, *24*(3), 241–259. https://doi.org/10.1175/1520-0469(1967)024<0241:teotaw>2.0.co;2

Match, A., & Fueglistaler, S. (2021). Large internal variability Dominates over global warming signal in observed lower stratospheric QBO amplitude. *Journal of Climate*, *34*(24), 9823–9836. https://doi.org/10.1175/jcli-d-21-0270.1

Meetham, A. R., & Dobson, G. M. (1937). The correlation of the amount of ozone with other characteristics of the atmosphere. *Quarterly Journal of the Royal Meteorological Society*, *63*(271), 289–307. https://doi.org/10.1002/QJ.49706327102

Meng, L., Liu, J., Tarasick, D. W., Randel, W. J., Steiner, A. K., Wilhelmsen, H., et al. (2021). Continuous rise of the tropopause in the northern hemisphere over 1980–2020. *Science Advances*, *7*(45), 8065. https://doi.org/10.1126/sciadv.abi8065

Meul, S., Langematz, U., Oberländer, S., Garny, H., & Jöckel, P. (2014). Chemical contribution to future tropical ozone change in the lower stratosphere. *Atmospheric Chemistry and Physics*, *14*(6), 2959–2971. https://doi.org/10.5194/acp-14-2959-2014

Neu, J. L., & Plumb, R. A. (1999). Age of air in a "leaky pipe" model of stratospheric transport. *Journal of Geophysical Research*, *104*(D16), 19243–19255. https://doi.org/10.1029/1999jd900251

Oberländer-Hayn, S., Gerber, E. P., Abalichin, J., Akiyoshi, H., Kerschbaumer, A., Kubin, A., et al. (2016). Is the Brewer-Dobson circulation increasing, or moving upward? *Geophysical Research Letters*, *43*(4), 1772–1779. https://doi.org/10.1002/2015GL067545

Oman, L. D., Plummer, D. A., Waugh, D. W., Austin, J., Scinocca, J. F., Douglass, A. R., et al. (2010). Multimodel assessment of the factors driving stratospheric ozone evolution over the 21st century. *Journal of Geophysical Research*, *115*(D24), 24306. https://doi.org/10.1029/2010jd014362

Paynter, D. J., Rand, K., Horowitz, L. W., Naik, V., John, J. G., Blanton, C., et al. (2018). NOAA-GFDL GFDL-ESM4 model output prepared for CMIP6 RFMIP PICLIM-4xCO_2. *Earth System Grid Federation*. https://doi.org/10.22033/ESGF/CMIP6.11964

Petropavlovskikh, I., Godin-Beekmann, S., Hubert, D., Damadeo, R., Hassler, B., & Sofieva, V. (2019). SPARC/I03C/GAW report on long-Term ozone trends and uncertainties in the stratosphere (Tech. Rep.). SPARC/I03C/GAW. Retrieved from https://www.sparc-climate.org/publications/sparc-reports/sparc-report-no-9/

Pincus, R., Forster, P. M., & Stevens, B. (2016). The radiative forcing model Intercomparison project (RFMIP): Experimental protocol for CMIP6. *Geoscientific Model Development*, *9*(9), 3447–3460. https://doi.org/10.5194/GMD-9-3447-2016

Plumb, R. A. (1996). A "tropical pipe" model of stratospheric transport. *Journal of Geophysical Research*, *101*(D2), 3957–3972. https://doi.org/10.1029/95jd03002

Plummer, D. A., Scinocca, J. F., Shepherd, T. G., Reader, M. C., & Jonsson, A. I. (2010). Quantifying the contributions to stratospheric ozone changes from ozone depleting substances and greenhouse gases. *Atmospheric Chemistry and Physics*, *10*(18), 8803–8820. https://doi.org/10.5194/acp-10-8803-2010

Polvani, L. M., Abalos, M., Garcia, R., Kinnison, D., & Randel, W. J. (2018). Significant weakening of Brewer-Dobson circulation trends over the 21st century as a consequence of the montreal protocol. *Geophysical Research Letters*, *45*(1), 401–409. https://doi.org/10.1002/2017gl075345

Qin, Y., Klein, S. A., Zelinka, M. D., & Golaz, C. (2021). LLNL E3SM1.0 model output prepared for CMIP6 CFMIP AMIP-P4K. *Earth System Grid Federation*. https://doi.org/10.22033/ESGF/CMIP6.15130

Reed, R. J. (1950). The role of vertical motions in ozone-weather relationships. *Journal of the Atmospheric Sciences*, *7*(4), 263–267. https://doi.org/10.1175/1520-0469(1950)007<0263:trovmi>2.0.co;2

Santer, B. D., Sausen, R., Wigley, T. M., Boyle, J. S., AchutaRao, K., Doutriaux, C., & Taylor, K. E. (2003). Behavior of tropopause height and atmospheric temperature in models, reanalyses, and observations: Decadal changes. *Journal of Geophysical Research - D: Atmospheres*, *108*(1), 4002. https://doi.org/10.1029/2002jd002258

Schubert, S. D., & Munteanu, M.-J. (1988). An analysis of tropopause pressure and total ozone correlations. *Monthly Weather Review*, *116*(3), 569–582. https://doi.org/10.1175/1520-0493(1988)116<0569:aaotpa>2.0.co;2

Seferian, R. (2018a). CNRM-CERFACS CNRM-ESM2-1 model output prepared for CMIP6 CMIP for experiment abrupt-4xCO_2. *Earth System Grid Federation*. https://doi.org/10.22033/ESGF/CMIP6.3918

Seferian, R. (2018b). CNRM-CERFACS CNRM-ESM2-1 model output prepared for CMIP6 CMIP picontrol. *Earth System Grid Federation*. https://doi.org/10.22033/ESGF/CMIP6.4165

Seferian, R. (2019). CNRM-CERFACS CNRM-ESM2-1 model output prepared for CMIP6 RFMIP PICLIM-4xCO_2. *Earth System Grid Federation*. https://doi.org/10.22033/ESGF/CMIP6.9643

Seidel, D. J., & Randel, W. J. (2006). Variability and trends in the global tropopause estimated from radiosonde data. *Journal of Geophysical Research*, *111*(21), D21101. https://doi.org/10.1029/2006jd007363

Shepherd, T. G. (2008). Dynamics, stratospheric ozone, and climate change. *Atmosphere-Ocean*, *46*(1), 117–138. https://doi.org/10.3137/ao.460106

Singh, M. S., & O'Gorman, P. A. (2012). Upward shift of the atmospheric general circulation under global warming: Theory and simulations. *Journal of Climate*, *25*(23), 8259–8276. https://doi.org/10.1175/jcli-d-11-00699.1

SPARC. (2010). SPARC report No. 5.

Steinbrecht, W., Claude, H., Köhler, U., & Hoinka, K. P. (1998). Correlations between tropopause height and total ozone: Implications for long-term changes. *Journal of Geophysical Research*, *103*(D15), 19183–19192. https://doi.org/10.1029/98jd01929

Stolarski, R. S., Waugh, D. W., Wang, L., Oman, L. D., Douglass, A. R., & Newman, P. A. (2014). Seasonal variation of ozone in the tropical lower stratosphere: Southern tropics are different from northern tropics. *Journal of Geophysical Research: Atmospheres*, *119*(10), 6196–6206. https://doi.org/10.1002/2013jd021294

Thompson, A. M., Stauffer, R. M., Wargan, K., Witte, J. C., Kollonige, D. E., & Ziemke, J. R. (2021). Regional and seasonal trends in tropical ozone from SHADOZ profiles: Reference for models and satellite products. *Journal of Geophysical Research: Atmospheres*, *126*(22), e2021JD034691. https://doi.org/10.1029/2021jd034691

Vallis, G. K., Zurita-Gotor, P., Cairns, C., & Kidston, J. (2015). Response of the large-scale structure of the atmosphere to global warming. *Quarterly Journal of the Royal Meteorological Society*, *141*(690), 1479–1501. https://doi.org/10.1002/qj.2456.1002/qj.2456

Voldoire, A. (2019a). Cnrm-CERFACS CNRM-CM6-1 model output prepared for CMIP6 CFMIP AMIP-P4K. *Earth System Grid Federation*. https://doi.org/10.22033/ESGF/CMIP6.3938

Voldoire, A. (2019b). CNRM-CERFACS CNRM-CM6-1 hr model output prepared for CMIP6 CMIP AMIP. *Earth System Grid Federation*. https://doi.org/10.22033/ESGF/CMIP6.3923

Waugh, D. W., Oman, L., Kawa, S. R., Stolarski, R. S., Pawson, S., Douglass, A. R., et al. (2009). Impacts of climate change on stratospheric ozone recovery. *Geophysical Research Letters*, *36*(3). https://doi.org/10.1029/2008gl036223

Webb, M. J., Andrews, T., Bodas-Salcedo, A., Bony, S., Bretherton, C. S., Chadwick, R., et al. (2017). The Cloud Feedback Model Intercomparison Project (CFMIP) contribution to CMIP6. *Geoscientific Model Development*, *10*(1), 359–384. https://doi.org/10.5194/GMD-10-359-2017

Wild, O. (2007). Modelling the global tropospheric ozone budget: Exploring the variability in current models. *Atmospheric Chemistry and Physics*, *7*(10), 2643–2660. https://doi.org/10.5194/ACP-7-2643-2007

Xian, T., & Homeyer, C. R. (2019). Global tropopause altitudes in radiosondes and reanalyses. *Atmospheric Chemistry and Physics*, *19*(8), 5661–5678. https://doi.org/10.5194/ACP-19-5661-2019

Yukimoto, S., Koshiro, T., Kawai, H., Oshima, N., Yoshida, K., Urakawa, S., et al. (2019a). Mri MRI-ESM2.0 model output prepared for CMIP6 CFMIP AMIP-P4K. *Earth System Grid Federation*. https://doi.org/10.22033/ESGF/CMIP6.6771

Yukimoto, S., Koshiro, T., Kawai, H., Oshima, N., Yoshida, K., Urakawa, S., et al. (2019b). MRI MRI-ESM2.0 model output prepared for cmip6 cmip abrupt-4xCO_2. *Earth System Grid Federation*. https://doi.org/10.22033/ESGF/CMIP6.6755

Yukimoto, S., Koshiro, T., Kawai, H., Oshima, N., Yoshida, K., Urakawa, S., et al. (2019c). MRI MRI-ESM2.0 model output prepared for CMIP6 CMIP AMIP. *Earth System Grid Federation*. https://doi.org/10.22033/ESGF/CMIP6.6758

Yukimoto, S., Koshiro, T., Kawai, H., Oshima, N., Yoshida, K., Urakawa, S., et al. (2019d). MRI MRI-ESM2.0 model output prepared for CMIP6 CMIP picontrol. *Earth System Grid Federation*. https://doi.org/10.22033/ESGF/CMIP6.6900

Yukimoto, S., Koshiro, T., Kawai, H., Oshima, N., Yoshida, K., Urakawa, S., et al. (2019e). MRI MRI-ESM2.0 model output prepared for CMIP6 RFMIP PICLIM-4xCO_2. *Earth System Grid Federation*. https://doi.org/10.22033/ESGF/CMIP66873